



Geophysical Research Letters*



RESEARCH LETTER

10.1029/2023GL103958

Key Points:

- Interannual variations of mean currents and eddies in the Caribbean Sea are linked to El Niño-Southern Oscillation (ENSO)
- ENSO-induced wind pattern changes modulate the north-south sea surface height differences and hence the mean currents in the Caribbean Sea
- Interannual variation of eddy kinetic energy in the Caribbean Sea is controlled by baroclinic instability

Supporting Information:

Supporting Information may be found in the online version of this article.

Correspondence to:

M. Huang, minghaih@udel.edu

Citation:

Huang, M., Liang, X., Yang, Y., & Zhang, Y. (2023). ENSO modulates mean currents and mesoscale eddies in the Caribbean Sea. *Geophysical Research Letters*, 50, e2023GL103958. https://doi.org/10.1029/2023GL103958

Received 4 APR 2023 Accepted 26 JUL 2023

© 2023. The Authors. This is an open access article under the terms of the Creative Commons Attribution License, which permits use, distribution and reproduction in any medium, provided the original work is properly cited.

ENSO Modulates Mean Currents and Mesoscale Eddies in the Caribbean Sea

Minghai Huang¹, Xinfeng Liang¹, Yang Yang², and Yang Zhang¹

¹School of Marine Science and Policy, University of Delaware, Lewes, DE, USA, ²State Key Laboratory of Marine Environmental Science, College of Ocean and Earth Sciences, Xiamen University, Xiamen, China

Abstract Although El Niño-Southern Oscillation (ENSO) and its global impacts through teleconnection have been known for decades, if and how the mean currents and mesoscale eddies in the Caribbean Sea are linked to ENSO remains an open question. Here, by analyzing satellite observations and an ocean reanalysis product, we found a close connection between mean currents, eddies in the Caribbean Sea and ENSO on interannual timescales. Strong El Niño events result in enhanced north-south sea surface height differences and consequently stronger mean currents in the Caribbean Sea, and the opposite happens during La Niña events. The eddy kinetic energy responds to ENSO via eddy-mean flow interaction, primarily through baroclinic instability, which releases the available potential energy stored in the mean currents to mesoscale eddies. Our results suggest some predictability of the mean currents and eddies in the Caribbean Sea, particularly during strong El Niño and La Niña events.

Plain Language Summary We explored the potential impacts of El Niño-Southern Oscillation (ENSO) on the circulation and mesoscale eddies in the Caribbean Sea. We found ENSO-related synchronized changes in mean currents and eddies across the entire Caribbean Sea. The connection between mean currents and ENSO is established through ENSO's impact on the north-south sea surface height (SSH) difference in the Caribbean Sea, which determines the strength of the geostrophic jet. During strong El Niño events, the easterly wind anomalies will increase the north-south SSH difference through Ekman transport, and consequently generate stronger mean currents. During strong La Niña events, the opposite happens. Through baroclinic instability, available potential energy stored in the mean currents will be transferred to eddies and results in ENSO-modified interannual variations of eddy kinetic energy. Our results suggest that interannual variations of mean currents and eddies in the Caribbean Sea might be predictable, particularly during strong El Niño and La Niña events.

1. Introduction

The Caribbean Sea is a critical region connecting the tropical Atlantic, the Gulf of Mexico (GoM), and the North Atlantic Ocean. The mean circulation in the Caribbean Sea is characterized by currents from the Lesser Antilles to the Yucatan Channel and into the GoM (Gordon, 1967; Johns et al., 2002) and is a major pathway for transporting mass, heat, salt, and other tracers in the Atlantic Circulation System. Mesoscale eddies are also ubiquitous in the Caribbean Sea (Centurioni & Niiler, 2003; Jouanno et al., 2012; López-Álzate et al., 2022; Pratt & Maul, 2000; van der Boog et al., 2019a, 2019b). These eddies advect cold filaments, modulate heat balance in the interior of the Caribbean Sea, and affect the temperature variability through the upwelling in the Cariaco Basin (Astor et al., 2003; Jouanno & Sheinbaum, 2013). They also transport nutrients, chlorophyll, *Sargassum*, larvae, and pollutants, and hence impact the marine ecosystem in the Caribbean Sea (Andrade & Barton, 2005; Chérubin & Richardson, 2007; E. M. Johns et al., 2014; Andrade-Canto et al., 2022). In addition, some studies suggest that the eddies in the Caribbean Sea could impact the eddy-shedding of the Loop Current in the GoM (e.g., Andrade-Canto et al., 2020; Huang et al., 2021; Laxenaire et al., 2023; Murphy et al., 1999; Ntaganou et al., 2023; Oey, 2004; Yang et al., 2020).

Some aspects of the interannual variability of mean currents and eddies in the Caribbean Sea have been studied. For instance, previous studies indicate that interannual variations of the Caribbean Current are related to the north–south sea surface height (SSH) difference, which is driven by the changing wind pattern (Alvera-Azcárate et al., 2009). In addition, baroclinic and barotropic instabilities of the mean current can affect the Caribbean eddies (Andrade & Barton, 2000; Carton & Chao, 1999; Jouanno et al., 2009, 2012; Richardson, 2005). In the

HUANG ET AL. 1 of 10

central Caribbean Sea (Colombia Basin), Jouanno et al. (2012) show that mean kinetic energy (MKE) and eddy kinetic energy (EKE) are related and exhibit a close relationship with wind stress. Moreover, a recent study using Self-Organizing Maps reveals interannual EKE variabilities in the Caribbean Sea, but no further investigation of the underlying mechanisms has been conducted (López-Álzate et al., 2022).

El Niño-Southern Oscillation (ENSO) teleconnection and its impacts on remote regions have been known for decades (Alexander et al., 2002; Yeh et al., 2018). In the Caribbean Sea, previous studies show that ENSO can affect wind stress, temperature, rainfall pattern, net primary production, and chlorophyll (e.g., Chang & Oey, 2013; Enfield & Mayer, 1997; Giannini et al., 2001; Maldonado et al., 2016; Malmgren et al., 1998; Muller-Karger et al., 2019; Sayol et al., 2022; Taylor et al., 2012). Early studies based on tide gauges and altimetry also suggest that interannual variations of sea level in the Caribbean Sea are correlated with ENSO (Alvera-Azcárate et al., 2009; Palanisamy et al., 2012). Some recent studies also directly link the interannual anomalous wind pattern in the Caribbean region to ENSO (Dong et al., 2022; Sayol et al., 2022).

As mentioned above, ENSO can modulate various quantities in the Caribbean Sea, such as winds stress and sea level. But how the mean currents and mesoscale eddies in the Caribbean Sea respond to ENSO have not been directly investigated. Two related questions also naturally arise: (a) Will ENSO-induced wind stress and sea level variations result in changes in the geostrophic jet i.e., driven by the north–south SSH difference? (b) How do mesoscale eddies in the Caribbean Sea respond to the variations of mean currents? In this study, we will try to answer these questions by analyzing altimetry observations and oceanic reanalysis products. We will focus on possible roles of ENSO in modulating the MKE and EKE in the whole Caribbean Sea. The rest of the paper is organized as follows: Section 2 describes the data and methods used in this study. Section 3 presents the results of the interannual variations of MKE, EKE, their relationships with ENSO, and the underlying mechanisms. The results are summarized and discussed in Section 4.

2. Data and Methods

2.1. Data

Satellite altimetry products, including sea level anomalies (SLA), absolute dynamic topography, and geostrophic currents, are used to characterize the surface eddy characteristics and validate the ocean reanalysis products. These products are distributed by the Copernicus Marine Environment Monitoring Service (CMEMS). The altimetry data has $0.25^{\circ} \times 0.25^{\circ}$ horizontal resolution and daily temporal intervals. The altimetry data from 1993 to 2020 are used in this study. And the SLA is referenced to a 20-year (1993–2012) mean (Pujol et al., 2016).

A global ocean reanalysis product, the Forecast Ocean Assimilation Model from Met Office (FOAM; Blockley et al., 2014), is used to describe and understand the interannual variations of mean currents and eddies. Forecast Ocean Assimilation Model from Met Office is distributed by the CMEMS Global Ocean Ensemble Reanalysis project. It is a homogeneous 3D gridded description of the physical state of the ocean constrained with satellite and in situ observations (Blockley et al., 2014). It has a temporal range from 1993 to 2020 and a daily temporal resolution. It has $0.25^{\circ} \times 0.25^{\circ}$ horizontal resolution and 75 vertical levels. The vertical resolution varies from a few meters near the sea surface to ~200 m near the bottom. Forecast Ocean Assimilation Model from Met Office was recently utilized in a similar study in the nearby North Brazil region (Huang et al., 2023) and reproduces the mean currents and eddy variabilities in the Caribbean Sea reasonably well (shown later in Section 3). Note that other ocean reanalyzes were also used to conduct similar analyses, and the conclusions are generally similar to the FOAM results. See Text S1, Table S1 and Figure S1 in Supporting Information S1 for more information.

Monthly averaged surface 10 m wind velocity from the European Centre for Medium-Range Weather Forecasts Reanalysis (Hersbach et al., 2020) is used to explore the possible forcing for the variations in mean currents and mesoscale eddies. The temporal range of the wind data is from 1993 to 2020. It has a $0.25^{\circ} \times 0.25^{\circ}$ horizontal resolution.

The daily sea surface temperature (SST) reprocessed product (Good et al., 2020) is also used. It has a $0.05^{\circ} \times 0.05^{\circ}$ horizontal resolution. Niño3.4, North Atlantic Oscillation (NAO) as well as Atlantic Multi-decadal Oscillation (AMO) indices are used to explore the relationships of various climate variabilities with mean currents and eddies in the Caribbean Sea. To be consistent with other datasets, time ranges of SST and climate indices used in this study are from 1993 to 2020.

HUANG ET AL. 2 of 10

2.2. Analyses

A recently developed time-varying multiscale energetics framework (Liang, 2016) is used to investigate the mean currents and eddy variabilities in the Caribbean Sea as well as the underlying mechanisms. This multiscale energetics framework is based on a new functional analysis apparatus, namely the multiscale window transform (MWT, Liang & Anderson, 2007). A brief description of this method is provided below and for more detailed information refer to Liang (2016) or Huang et al. (2023).

MWT is developed for a faithful representation of localized multiscale energetics on the scale windows (Liang & Anderson, 2007). With MWT, we can decompose a function space into a direct sum of orthogonal subspaces while retaining its temporal locality. For instance, a flow filed u = u(t) can be decomposed into a nonstationary mean component $u^{\sim 0}(t)$ and an eddy component $u^{\sim 1}(t)$. $u^{\sim \varpi}(t)$, like a filtered series, is called the multiscale window reconstruction of u(t) on the scale window $\varpi(\varpi = 0, 1)$. Corresponding to each reconstruction $u^{\sim \varpi}(t)$, there exists a transform coefficient $\hat{u}_n^{\sim \varpi}$, where $\widehat{(\cdot)}_n^{\sim \varpi}$ denotes MWT on window ϖ at time step n. The energy on scale window $\varpi = (0, 1)$ proves to be proportional to $(\hat{u}_n^{\sim \varpi})^2$.

Under the MWT framework, kinetic energy (KE) and available potential energy (APE) on scale window ϖ can be defined as:

$$K^{\varpi} = \frac{1}{2} \hat{\boldsymbol{p}}_{h}^{\sim \varpi} \cdot \hat{\boldsymbol{p}}_{h}^{\sim \varpi}, \tag{1}$$

$$A^{\varpi} = \frac{1}{2}c\left(\hat{\rho}^{\sim\varpi}\right)^2,\tag{2}$$

where v_h is the horizontal velocity, $c = g^2/\rho_0^2 N^2$, N is the Brunt–Väisälä frequency. ρ is the density anomaly (with the mean vertical profile $\rho(z)$ removed). $\varpi = 0$, 1 stands for the mean current and eddy window, respectively. Here, K^0 and K^1 represent MKE and EKE, respectively. It should be noted that both K^0 and K^1 will vary with time.

The MWT-based multiscale ocean energetic equations for the multiscale KE (K^{ϖ}) and available potential energy (APE, A^{ϖ}) can be described as:

$$\frac{\partial K^{\varpi}}{\partial t} = \underbrace{-\nabla \cdot \left[\frac{1}{2}\left[\widehat{(\mathbf{v}\mathbf{v}_{h})}^{\sim \varpi} \cdot \widehat{\mathbf{v}}_{h}^{\sim \varpi}\right]\right]}_{-\nabla \cdot Q_{k}^{\varpi}} + \underbrace{\frac{1}{2}\left[\widehat{(\mathbf{v}\mathbf{v}_{h})}^{\sim \varpi} : \nabla \widehat{\mathbf{v}}_{h}^{\sim \varpi} - \nabla \cdot \widehat{(\mathbf{v}\mathbf{v}_{h})}^{\sim \varpi} \cdot \mathbf{v}_{h}^{\sim \varpi}\right]}_{\Gamma_{k}^{\varpi}} \\
-\nabla \cdot \left(\frac{1}{\rho_{0}}\widehat{\mathbf{v}}^{\sim \varpi}\widehat{\mathbf{P}}^{\sim \varpi}\right) + \underbrace{\left(-\frac{g}{\rho_{0}}\widehat{\rho}^{\sim \varpi}\widehat{\mathbf{w}}^{\sim \varpi}\right)}_{b^{\varpi}} + F_{K}^{\varpi}, \tag{3}$$

$$\frac{\partial A^{\varpi}}{\partial t} = \underbrace{-\nabla \cdot \left[\frac{1}{2}c\hat{\rho}^{\sim\varpi}(\widehat{\mathbf{v}}\hat{\rho})^{\sim\varpi}\right]}_{-\nabla \cdot Q_{A}^{\varpi}} + \underbrace{\frac{c}{2}\left[(\widehat{\mathbf{v}}\hat{\rho})^{\sim\varpi} \cdot \nabla\hat{\rho}^{\sim\varpi} - \rho^{\sim\varpi}\nabla \cdot (\widehat{\mathbf{v}}\hat{\rho})^{\sim\varpi}\right]}_{\Gamma_{A}^{\varpi}} + \underbrace{\frac{g}{\rho_{0}}\hat{\rho}^{\sim\varpi}\widehat{\mathbf{w}}^{\sim\varpi}}_{-b^{\varpi}} + \underbrace{\frac{1}{2}\hat{\rho}^{\sim\varpi}(\widehat{\mathbf{w}}\hat{\rho})^{\sim\varpi}}_{S_{A}^{\varpi}} + F_{A}^{\varpi}, \tag{4}$$

Variabilities of KE (K) and APE (A) on the left side are controlled by the dynamics processes on the right side, where $-\nabla \cdot Q_k^\varpi$ and $-\nabla \cdot Q_A^\varpi$ are the advection of K^ϖ and A^ϖ , respectively. $-\nabla \cdot Q_P^\varpi$ is the pressure flux convergence. Γ_k^ϖ and Γ_A^ϖ are cross-scale transfers of KE and APE to window ϖ from other windows, standing for the redistribution of energy among different scales. $\Gamma_k^{0\to 1}$ and $\Gamma_A^{0\to 1}$ are barotropic transfer (BT) and baroclinic transfer (BC), respectively. The b^ϖ terms are the buoyancy conversion between KE and APE. S_A^ϖ is the result from the vertical shear of c (a source/sink of A^ϖ). F_K^ϖ and F_A^ϖ are residual terms including contributions from dissipation, external forcing, and subgrid processes. Detailed expressions and meanings of the symbols are listed in Table S2 in Supporting Information S1.

To separate mean currents and eddies with the MWT approach, an eddy scale level or a cutoff period needs to be determined. Early numerical studies in the Caribbean Sea set the mesoscale window shorter than 120 or

HUANG ET AL. 3 of 10

125 days (Jouanno et al., 2012; van der Boog et al., 2019b). Recently, based on 27 years of satellite altimetry data, López-Álzate et al. (2022) identified that the average lifetime for all the eddies in the Caribbean Sea is 62 ± 37 days (mean \pm standard deviation) and most of them (~90%) have a lifetime shorter than 160 days. Therefore, a period shorter than 160 days appears to be an appropriate choice for the cut-off period of the mesoscale window. We also tested ~120 days as the scale level, and the results are quantitatively similar.

To further explore how ENSO modulates the mean currents and eddies, potential factors like wind velocity, SST, SLA, and geostrophic currents in the Caribbean Sea are linearly regressed into the Niño3.4 index. The representation of a simple linear regression is $Y = \beta_0 + \beta_1 X$, where Y is a dependent variable, β_0 , β_1 are the regression coefficients, X is an independent variable. In this study, X represents the normalized Niño3.4 index (with its mean being subtracted and then being divided by its standard deviation) and Y is one of the few variables mentioned above. Since we in this study focused on the role of ENSO, monthly climatology and linear trends are removed and a 2-year lowpass filter is applied before the regressions. We also tested 1- and 3-year lowpass filters, and the results are similar.

3. Results

MKE and EKE in the Caribbean Sea from the altimetry and FOAM are shown in Figure 1. We first examine to what extent the altimetry and FOAM results agree. Mean currents from the altimetry and FOAM, displayed as high MKE from the Lesser Antilles to the Yucatan Channel, have similar spatial distribution (Figures 1a and 1b). In the three basins (i.e., the Colombia Basin, the Venezuela Basin, and the Cayman Basin), similar interannual variabilities (Figures 1e-1g) and significantly high correlations between altimetry and FOAM MKEs also appear. For the EKE (Figures 1i-1k), temporal evolutions of FOAM EKE and altimetry EKE agree reasonably well. Note that values of MKE and EKE from FOAM are generally smaller than altimetry results, which are likely due to the relatively low-resolution of FOAM (Text S2 in Supporting Information S1). Nevertheless, good agreements of temporal variations of MKE/EKE from the altimetry and FOAM suggest that FOAM can be used to examine interannual variations of mean currents and eddies in the Caribbean Sea, as well as the underlying mechanisms.

We then examine the evolutions of MKE and EKE in the three basins of the Caribbean Sea. We first look at the MKE (Figures 1e-1g). Evident synchronized interannual variations of MKE among the three basins are presented in both altimetry and FOAM. More specifically, in all the three basins, high MKE appears in 1994–1995, 1997–1998, 2015–2016, 2019–2020, and low MKE appears in 1993–1994, 1999–2000, 2017–2018, and 2020–2021. The synchronized variations of MKE are also reflected in high correlations of MKE in different ocean basins, with 0.74 between the Colombia and Venezuela Basins, and 0.77 between the Colombia and Cayman Basins. For EKE, similar synchronized temporal variations revealed in MKE are also exhibited. The EKE correlation coefficients are 0.71 between the Colombia and Venezuela Basins, and 0.71 between the Colombia and Cayman Basins. In addition, higher MKE/EKE in 1997–1998, 2015–2016 (strong El Niño events), and lower MKE/EKE in 2020–2021 (one strong La Niña event) suggest an important role of ENSO on the interannual variations of the mean currents and eddies in the Caribbean Sea. This is further confirmed by significantly high correlations between Niño3.4 and MKE/EKE in the three basins (Table S3 in Supporting Information S1).

Besides ENSO, we also examine correlations between NAO, AMO and MKE/EKE in the Caribbean Sea (Table S3 in Supporting Information S1). The results show that their relationships are not as substantial as ENSO, and in many cases not even statistically significant. For instance, the altimetry MKE in the Colombia Basin shows much lower correlation coefficients, with \sim 0.2 for NAO and \sim -0.3 for AMO, and the corresponding FOAM MKE in the Colombia Basin is not significantly correlated with either NAO or AMO. For EKE, the relationships with NAO and AMO are even less clear. So, NAO and AMO likely play minor roles in modulating the MKE and EKE in the Caribbean Sea, and we will focus on the effects of ENSO in the rest of this paper.

We then investigate how mean currents and eddies in the Caribbean Sea are modulated by ENSO. First, we look at the mean states of the Caribbean Sea. Figure 2a shows that an intense and persistent easterly wind exists in the Caribbean Sea (Wang, 2007). This wind directly controls the intensity and occurrence of the upwelling in the southern Caribbean Sea (Montoya-Sánchez et al., 2018), which appears as a cold SST patch in Figure 2b. The easterly wind also drives the water to pile up in the northern Caribbean Sea through Ekman transport and contributes to the SSH difference between the north and south Caribbean Sea. And the mean currents in the Caribbean Sea are largely determined by the latitudinal gradients of the SSH (Figure 2c).

HUANG ET AL. 4 of 10

19448007, 2023, 15, Downloaded from https://agupubs.onlinelibrary.wiley.com/doi/10.1029/2023GL103958, Wiley Online Library on [08/10/2023]. See the Terms and Conditions (https://onlinelibrary.wiley.com/ems-and-conditions) on Wiley Online Library for rules of use; OA

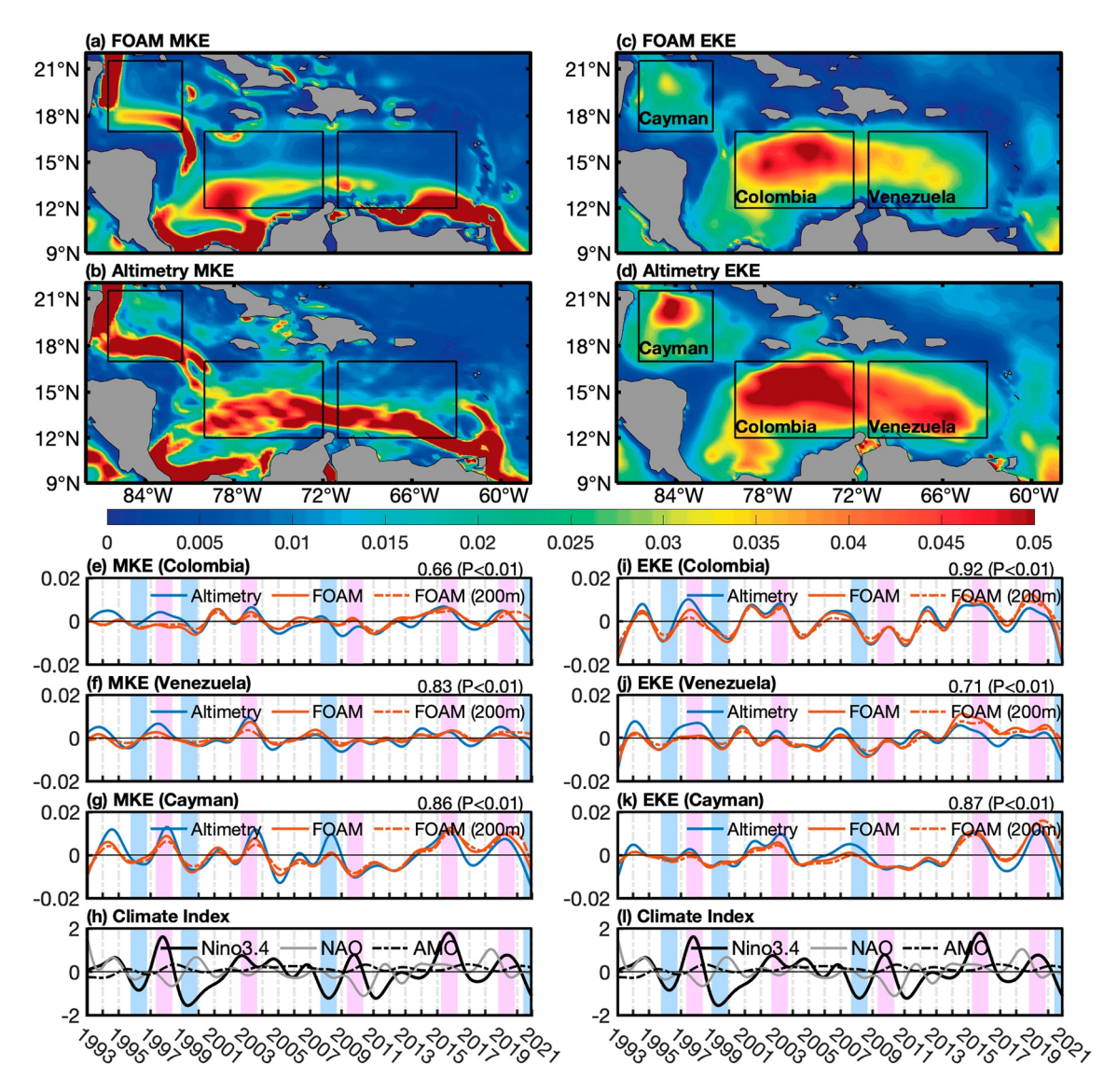


Figure 1. Spatial distribution of the time means of (a, b) mean kinetic energy (MKE, m^2 s⁻²) and (c, d) eddy kinetic energy (EKE, m^2 s⁻²) from FOAM and altimetry between 1993 and 2020. (e, i), (f, j), (g, k) 2-yr lowpass MKE and EKE (m^2 s⁻²) anomalies from altimetry and FOAM over the Colombia, the Venezuela and the Cayman Basin, respectively. Correlation coefficients between altimetry and FOAM as well as the corresponding *p*-values are noted in the top right of each panel. Note that orange dashed lines represent depth-mean (upper 200 m) results from FOAM. The bottom panels (h, l) show the 2-yr lowpass-filtered Niño3.4, NAO, and AMO indices. Bars in panels (e–l) mark El Niño (pink) and La Niña (light blue) events.

We then regress the wind velocity, SST, and SSH anomalies (SSHA) onto the normalized Niño3.4 index (Figures 2d–2f). The regression analysis shows that positive Niño3.4 indices (El Niño) are associated with an anticyclonic wind anomaly in the Caribbean Sea (Figure 2d). During El Niño, positive SST anomalies in the central-eastern Pacific lead to the shift of the Walker Circulation to the central-eastern Pacific. More intense easterly wind anomalies will occur in the Caribbean region. This wind pattern will drive an oceanic convergence and hence higher sea levels in the northern Caribbean Sea. In the meantime, the easterly wind anomalies in the southern Caribbean Sea can intensify the regional upwelling (Figure 2e). As a consequence, the north-south SSH difference in the Caribbean Sea will increase during El Niño events and strengthen the mean currents through geostrophic balance (Figure 2f). During La Niña events, on the contrary, negative SST anomalies in the eastern Pacific are associated with an enhanced downward branch of the Walker Circulation. In the Caribbean region, this is characterized by westerly wind anomalies at surface levels. As a consequence, the upwelling in the southern Caribbean Sea is suppressed (Sayol et al., 2022), north-south SSH difference decreases, and the mean currents in the Caribbean Sea are weakened.

HUANG ET AL. 5 of 10

19448007, 2023, 15, Downloaded from https://agupubs.onlinelibrary.wiley.com/doi/10.1029/2023GL103958, Wiley Online Library on [08/10/2023]. See the Terms and Conditions (https://online.com/doi/10.1029/2023GL103958, Wiley Online Library on [08/10/2023]. See the Terms and Conditions (https://online.com/doi/10.1029/2023GL103958, Wiley Online Library on [08/10/2023]. See the Terms and Conditions (https://online.com/doi/10.1029/2023GL103958, Wiley Online Library on [08/10/2023]. See the Terms and Conditions (https://online.com/doi/10.1029/2023GL103958, Wiley Online Library on [08/10/2023]. See the Terms and Conditions (https://online.com/doi/10.1029/2023GL103958, Wiley Online Library on [08/10/2023]. See the Terms and Conditions (https://online.com/doi/10.1029/2023GL103958, Wiley Online Library on [08/10/2023]. See the Terms and Conditions (https://online.com/doi/10.1029/2023GL103958, Wiley Online Library on [08/10/2023].

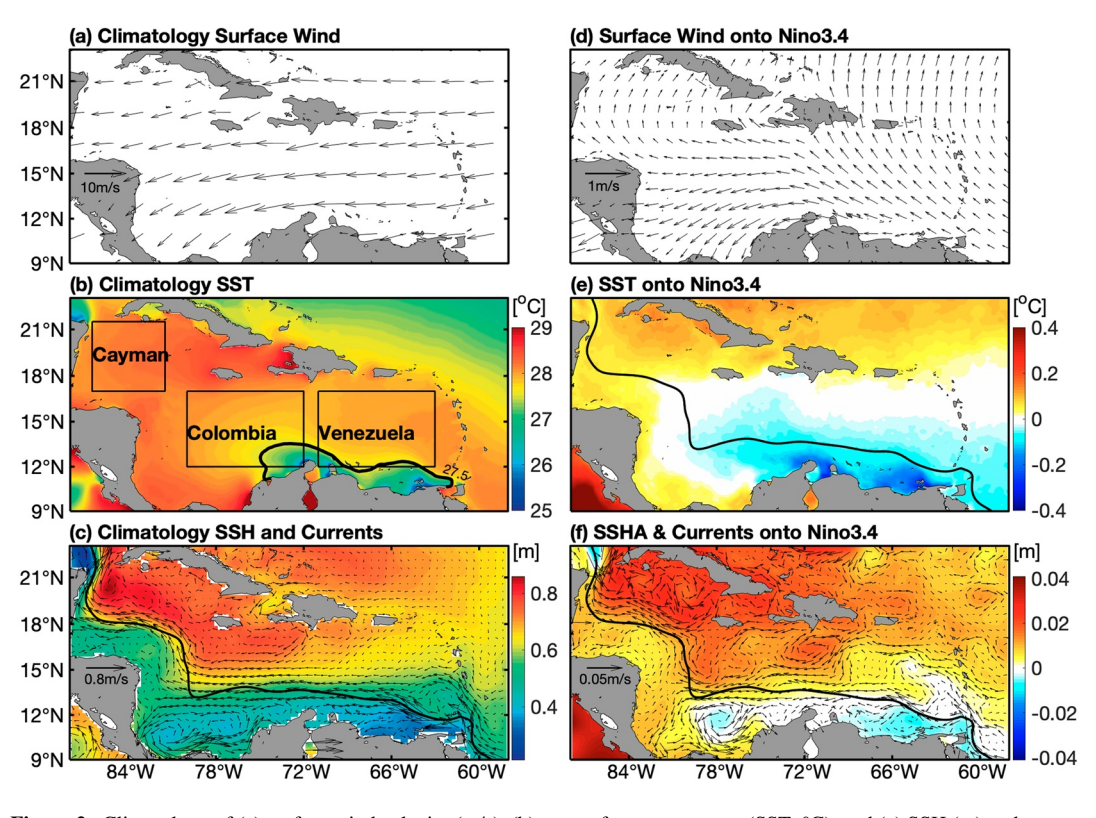


Figure 2. Climatology of (a) surface wind velocity (m/s), (b) sea surface temperature (SST; °C), and (c) SSH (m) and geostrophic currents (m/s) between 1993 and 2020. Spatial distribution of linear regression coefficients of (d) Wind velocity (e) SST, and (f) SSHA and currents onto the normalized Niño3.4 index. The black solid curve in (c, e, f) represents the maximum speed of the climatology mean current. The 27.5°C contour line in (b) roughly marks the boundary of the upwelling region in the Caribbean Sea.

Correlation coefficients between the Niño3.4 index and MKE/EKE from altimetry and FOAM are also directly calculated and displayed in Figure 3. Significant and high correlations between the Niño3.4 index and MKE/EKE over the Caribbean Sea are shown in both products. For the MKE, the highest correlations are primarily confined along the mean current (Figures 3a–3c). As suggested above, the synchronized MKE evolution with ENSO in the whole Caribbean Sea is established through ENSO's impacts on the north-south SSH differences and hence the geostrophic currents. Like the MKE, the EKE in the Caribbean Sea also exhibits synchronized variability with the Niño3.4 index but their responses are not confined along the mean current but cover a much larger area (Figures 3d–3f).

We then explore the underlying mechanisms for the effects of ENSO on the interannual variability of EKE in the Caribbean Sea. Temporal evolutions of EKE and the related dynamic processes over the three Caribbean basins are displayed in Figure 4. The high correlations between baroclinic transfer (BC, $\Gamma_A^{0\to 1}$) and EKE as well as between buoyancy conversion (b^1) and EKE indicate that baroclinic instability dominates the EKE variability. The BT ($\Gamma_k^{0\to 1}$) also exhibits positive correlation with the EKE, but its magnitude is much smaller than the BC term (Figure S2 in Supporting Information S1). The nonlocal term (combined effect of advection and pressure work) is negatively correlated with the EKE, suggesting that EKE generated through the instability processes is damped by nonlocal processes via advection and pressure work.

The correlation coefficients between the Niño3.4 index and each of the four budget terms are also calculated (Figure 4). The baroclinic transfer and buoyancy conversion are consistently more closely related to ENSO than the barotropic term. The nonlocal process is always negatively related to Niño3.4. For instance, in the most energetic Colombia Basin (Figure 4a), the correlation coefficient between the Niño3.4 index and BC is 0.51, but the correlation coefficient between the Niño3.4 index and BT is 0.06, indicating that the effect of ENSO on EKE is mainly through baroclinic instabilities in that basin. In the classical instability formalism, baroclinic instability is proportional to the vertical shear of the horizontal flow (Pedlosky, 1987). We hence check the correlation

HUANG ET AL. 6 of 10

1944/8007, 2023, 15, Downloaded from https://agupubs.onlinelibrary.wiley.com/doi/10.1029/2023GL103958, Wiley Online Library on [08/10/2023]. See the Terms and Conditions (https://onlinelibrary.wiley.com/terms-and-conditions) on Wiley Online Library for rules of use; OA articles are governed by the applicable Creative C

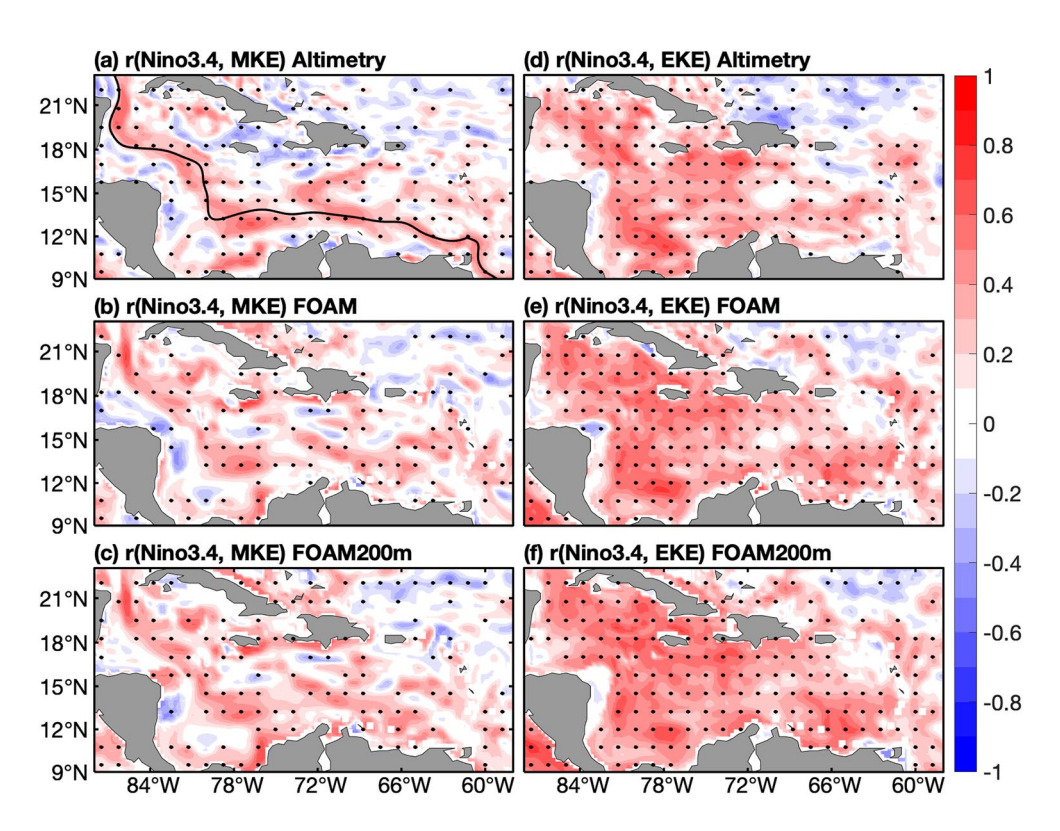


Figure 3. (a–c) Correlation coefficients between MKE and Niño3.4 index from (a) altimetry, (b) FOAM, (c) depth-mean (200 m) FOAM. (d–f) Same as (a–c), but for EKE. The black curve in (a) represents the maximum speed of the climatology mean current. Correlation coefficients above the 95% significance level are marked as black dots. All the time series are 2-yr lowpass filtered.

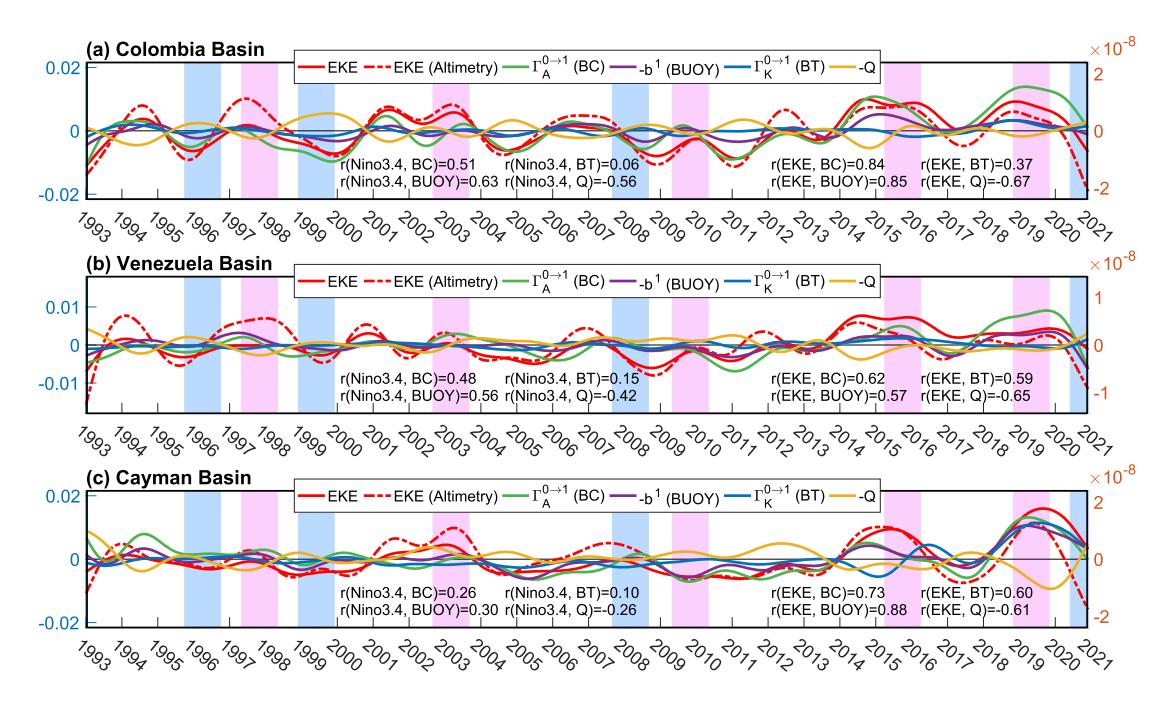


Figure 4. (a) Time series of the area-mean and depth-mean (upper 200 m) EKE and four dynamic processes over the Colombia Basin from FOAM. The terms are baroclinic transfer (BC, green), buoyancy conversion (buoy, purple), barotropic transfer (BT, blue), and nonlocal process (Q, yellow). Altimetry EKE (red dash) is also added for comparison. All the time series are 2-yr lowpass filtered. The units of the EKE budget terms and EKE are m² s⁻³ and m² s⁻², respectively. (b, c) As in (a), but for the Venezuela Basin and Cayman Basin, respectively. The correlation coefficients, r, between four dynamic processes, EKE and the Niño3.4 index are shown in the bottom of each panel. Bars in (a–c) represent El Niño (pink) and La Niña (blue) events.

HUANG ET AL. 7 of 10

between the vertical shear of the horizontal flow and the Niño3.4 index, and significant high correlations are found along the trajectory of the mean current in the Caribbean Sea (Figure S3 in Supporting Information S1). This further confirms that ENSO modulates EKE through its effect on the mean currents and energy transfer from the background currents to eddies through baroclinic instabilities.

4. Conclusions and Discussion

In this study, we found substantial and synchronized interannual variabilities of MKE and EKE in the whole Caribbean Sea. These interannual variabilities are also closely related to ENSO, indicating that ENSO can modulate the mean currents and mesoscale eddies in the Caribbean Sea. Note that these findings not only appear in FOAM but also in other reanalyzes products we examined (Figure S1 in Supporting Information S1). In addition, although previous studies showed significant dynamic differences between the three basins of the Caribbean Sea (e.g., Jouanno et al., 2008), the synchronized responses of mean currents and eddies to ENSO occur across the whole Caribbean Sea, suggesting that the dynamical separation of the three basins in the Caribbean Sea are timescale dependent.

The ENSO modulation of mean currents in the Caribbean Sea is established through ENSO's impacts on the north-south SSH differences in the Caribbean Sea, which through geostrophic balance affect the mean currents. During El Niño events, the easterly wind anomalies drive the water to pile up in the northern Caribbean Sea and lower the SSH in the southern Caribbean Sea through Ekman transport. These will lead to increased north-south SSH differences and strengthened the mean current, and during La Niña events the opposite happens. The interannual EKE variability is primarily controlled by baroclinic instability, which releases available potential energy stored in the mean currents to mesoscale eddies. Since the mean currents are modulated by ENSO, high correlations between ENSO and EKE are expected.

Besides ENSO, we also notice weak but, in some cases, significant correlations between MKE/EKE and other climate modes, such as NAO and AMO (Table S3 in Supporting Information S1). The altimetry data show that NAO is positively correlated with MKE/EKE, while AMO is negatively correlated. In particular, during a "moderate" El Niño event around 2010 (comparing to two "strong" El Niño events during 1997/1998 and 2015/2016), MKE and EKE did not show positive but negative anomalies. This could be related to the strong negative NAO and weak positive AMO, both of which induced negative MKE/EKE anomalies. In addition, effects of climate modes, such as ENSO, NAO, AMO, the Pacific Decadal Oscillation, and Pacific/North American Pattern on the Caribbean winds have been studied and the Niño3.4 index was found to be the dominant mode (Maldonado et al., 2016). This is consistent with our findings of the leading role of ENSO in modulating mean currents and eddies in the Caribbean Sea. Our results suggest some predictability of the mean current and mesoscale eddies in the Caribbean Sea, particularly during strong El Niño and La Niña events.

ENSO modulations of mean currents and eddies in the Caribbean Sea also have broader implications. For instance, ENSO can potentially affect the marine productivity in the Caribbean Sea. A high correlation between ENSO and chlorophyll in the upwelling region has been identified, suggesting that the upwelling modulated by ENSO could affect nutrients from deeper ocean and influence marine productivity (Figure S4 in Supporting Information S1). That said, many other factors, such as the Orinoco River discharge (e.g., Muller-Karger et al., 1989), also affect the marine productivity in the Caribbean Sea and the relationships between ENSO and marine productivity across the whole Caribbean Sea are likely more complex. In addition, previous studies (e.g., Huang et al., 2021; Laxenaire et al., 2023; Mildner et al., 2013; Oey, 2004) suggest that the mean currents and eddies in the Caribbean Sea could affect downstream regions, like the GoM and the Florida Current. So, ENSO-related interannual variations in the Caribbean Sea could potentially be advected downstream and result in regional interannual variability. All these questions are interesting and will be investigated in the future.

Data Availability Statement

All the data used in this study are publicly available. The satellite altimetry (https://doi.org/10.48670/moi-00145) and FOAM (https://doi.org/10.48670/moi-00024) model data set is from the Copernicus Marine Environment Monitoring Service (CMEMS, https://marine.copernicus.eu/). The sea surface temperature data is from CMEMS (https://doi.org/10.48670/moi-00168). The surface wind from the European Centre for Medium-Range Weather Forecasts (ECMWF) Reanalysis fifth Generation (ERA5) is available at (https://doi.org/10.24381/cds.f17050d7).

HUANG ET AL. 8 of 10



Geophysical Research Letters

10.1029/2023GL103958

The NAO (https://www.cpc.ncep.noaa.gov/products/precip/CWlink/pna/nao.shtml) and AMO index (https://psl.noaa.gov/data/correlation/amon.us.long.data) are from National Oceanic and Atmospheric Administration (NOAA). The Niño3.4 index is from Asia-Pacific Data-Research Center is available at (http://apdrc.soest.hawaii.edu/las/v6/dataset?catitem=1261).

Acknowledgments

We thank two anonymous reviewers whose comments and suggestions helped us improve this paper. The work was supported in part by National Science Foundation through Grant OCE-2122507.

References

- Alexander, M. A., Bladé, I., Newman, M., Lanzante, J. R., Lau, N.-C., & Scott, J. D. (2002). The atmospheric bridge: The influence of ENSO teleconnections on air–sea interaction over the global oceans. *Journal of Climate*, 15(16), 2205–2231. https://doi.org/10.1175/1520-0442(2002)015<2205:TABTIO>2.0.CO:2
- Alvera-Azcárate, A., Barth, A., & Weisberg, R. H. (2009). The surface circulation of the Caribbean Sea and the Gulf of Mexico as inferred from satellite altimetry. *Journal of Physical Oceanography*, 39(3), 640–657. https://doi.org/10.1175/2008JPO3765.1
- Andrade, C. A., & Barton, E. D. (2000). Eddy development and motion in the Caribbean Sea. *Journal of Geophysical Research*, 105(C11), 26191–26201. https://doi.org/10.1029/2000JC000300
- Andrade, C. A., & Barton, E. D. (2005). The Guajira upwelling system. Continental Shelf Research, 25(9), 1003–1022. https://doi.org/10.1016/j.csr.2004.12.012
- Andrade-Canto, F., Beron-Vera, F. J., Goni, G. J., Karrasch, D., Olascoaga, M. J., & Triñanes, J. (2022). Carriers of *Sargassum* and mechanism for coastal inundation in the Caribbean Sea. *Physics of Fluids*, 34(1), 016602. https://doi.org/10.1063/5.0079055
- Andrade-Canto, F., Karrasch, D., & Beron-Vera, F. J. (2020). Genesis, evolution, and apocalypse of Loop Current rings. *Physics of Fluids*, 32(11), 116603. https://doi.org/10.1063/5.0030094
- Astor, Y., Muller-Karger, F., & Scranton, M. I. (2003). Seasonal and interannual variation in the hydrography of the Cariaco Basin: Implications for basin ventilation. Continental Shelf Research, 23(1), 125–144. https://doi.org/10.1016/S0278-4343(02)00130-9
- Blockley, E. W., Martin, M. J., McLaren, A. J., Ryan, A. G., Waters, J., Lea, D. J., et al. (2014). Recent development of the Met Office operational ocean forecasting system: An overview and assessment of the new global FOAM forecasts. *Geoscientific Model Development*, 7(6), 2613–2638. https://doi.org/10.5194/gmd-7-2613-2014
- Carton, J. A., & Chao, Y. (1999). Caribbean Sea eddies inferred from TOPEX/Poseidon altimetry and a 1/6° Atlantic Ocean model simulation. Journal of Geophysical Research, 104(C4), 7743–7752. https://doi.org/10.1029/1998JC900081
- Centurioni, R., & Niiler, P. (2003). On the surface currents of the Caribbean Sea. Geophysical Research Letters, 30(6), 1279. https://doi.org/10.1029/2002GL016231
- Chang, Y.-L., & Oey, L.-Y. (2013). Coupled response of the trade wind, SST gradient, and SST in the Caribbean Sea, and the potential impact on Loop current's interannual variability. *Journal of Physical Oceanography*, 43(7), 1325–1344. https://doi.org/10.1175/JPO-D-12-0183.1
- Chérubin, L. M., & Richardson, P. L. (2007). Caribbean current variability and the influence of the Amazon and Orinoco freshwater plumes. Deep Sea Research Part I: Oceanographic Research Papers, 54(9), 1451–1473. https://doi.org/10.1016/j.dsr.2007.04.021
- Dong, S., Volkov, D. L., Goni, G., Pujiana, K., Tagklis, F., & Baringer, M. (2022). Remote impact of the equatorial Pacific on Florida current transport. *Geophysical Research Letters*, 49(4), e2021GL096944. https://doi.org/10.1029/2021GL096944
- Enfield, D. B., & Mayer, D. A. (1997). Tropical Atlantic sea surface temperature variability and its relation to El Niño-Southern Oscillation. *Journal of Geophysical Research*, 102(C1), 929–945. https://doi.org/10.1029/96JC03296
- Giannini, A., Cane, M. A., & Kushnir, Y. (2001). Interdecadal changes in the ENSO teleconnection to the Caribbean region and the North Atlantic Oscillation. *Journal of Climate*, 14(13), 2867–2879. https://doi.org/10.1175/1520-0442(2001)014<2867;ICITET>2.0.CO;2
- Good, S., Fiedler, E., Mao, C., Martin, M. J., Maycock, A., Reid, R., et al. (2020). The current configuration of the OSTIA system for operational production of foundation sea surface temperature and ice concentration analyses. *Remote Sensing*, 12(4), 720. https://doi.org/10.3390/rs12040720
- Gordon, A. L. (1967). Circulation of the Caribbean Sea. Journal of Geophysical Research, 72(24), 6207–6223. https://doi.org/10.1029/ 17072i024p06207
- Hersbach, H., Bell, B., Berrisford, P., Hirahara, S., Horányi, A., Muñoz-Sabater, J., et al. (2020). The ERA5 global reanalysis. *Quarterly Journal of the Royal Meteorological Society*, 146(730), 1999–2049. https://doi.org/10.1002/qj.3803
- Huang, M., Liang, X., Zhu, Y., Liu, Y., & Weisberg, R. H. (2021). Eddies connect the tropical Atlantic ocean and the Gulf of Mexico. *Geophysical Research Letters*, 48(4), e2020GL091277. https://doi.org/10.1029/2020GL091277
- Huang, M., Yang, Y., & Liang, X. (2023). Seasonal eddy variability in the northwestern tropical Atlantic Ocean. *Journal of Physical Oceanogra-phy*, 53(4), 1069–1085. https://doi.org/10.1175/JPO-D-22-0200.1
- Johns, E. M., Muhling, B. A., Perez, R. C., Müller-Karger, F. E., Melo, N., Smith, R. H., et al. (2014). Amazon River water in the northeast-ern Caribbean Sea and its effect on larval reef fish assemblages during April 2009. Fisheries Oceanography, 23(6), 472–494. https://doi.org/10.1111/fog.12082
- Johns, W. E., Townsend, T. L., Fratantoni, D. M., & Wilson, W. D. (2002). On the Atlantic inflow to the Caribbean Sea. *Deep Sea Research Part I: Oceanographic Research Papers*, 49(2), 211–243. https://doi.org/10.1016/S0967-0637(01)00041-3
- Jouanno, J., & Sheinbaum, J. (2013). Heat balance and eddies in the Caribbean upwelling system. Journal of Physical Oceanography, 43(5), 1004–1014. https://doi.org/10.1175/JPO-D-12-0140.1
- Jouanno, J., Sheinbaum, J., Barnier, B., & Molines, J.-M. (2009). The mesoscale variability in the Caribbean Sea. Part II: Energy sources. *Ocean Modelling*, 26(3–4), 226–239. https://doi.org/10.1016/j.ocemod.2008.10.006
- Jouanno, J., Sheinbaum, J., Barnier, B., Molines, J. M., & Candela, J. (2012). Seasonal and interannual modulation of the eddy kinetic energy in the Caribbean Sea. *Journal of Physical Oceanography*, 42(11), 2041–2055. https://doi.org/10.1175/JPO-D-12-048.1
- Jouanno, J., Sheinbaum, J., Barnier, B., Molines, J.-M., Debreu, L., & Lemarié, F. (2008). The mesoscale variability in the Caribbean Sea. Part I: Simulations and characteristics with an embedded model. *Ocean Modelling*, 23(3–4), 82–101. https://doi.org/10.1016/j.ocemod.2008.04.002
- Laxenaire, R., Chassignet, E. P., Dukhovskoy, D. S., & Morey, S. L. (2023). Impact of upstream variability on the Loop Current dynamics in numerical simulations of the Gulf of Mexico. Frontiers in Marine Science, 10, 1080779. https://doi.org/10.3389/fmars.2023.1080779
- Liang, X. S. (2016). Canonical transfer and multiscale energetics for primitive and quasigeostrophic atmospheres. *Journal of the Atmospheric Sciences*, 73(11), 4439–4468. https://doi.org/10.1175/JAS-D-16-0131.1
- Liang, X. S., & Anderson, D. G. M. (2007). Multiscale window transform. Multiscale Modeling and Simulation, 6(2), 437–467. https://doi.org/10.1137/06066895X

HUANG ET AL. 9 of 10

- López-Álzate, M. E., Sayol, J.-M., Hernández-Carrasco, I., Osorio, A. F., Mason, E., & Orfila, A. (2022). Mesoscale eddy variability in the Caribbean Sea. *Ocean Dynamics*, 72(9–10), 679–693. https://doi.org/10.1007/s10236-022-01525-9
- Maldonado, T., Rutgersson, A., Amador, J., Alfaro, E., & Claremar, B. (2016). Variability of the Caribbean low-level jet during boreal winter: Large-scale forcings: Caribbean low-level jet and its variability. *International Journal of Climatology*, 36(4), 1954–1969. https://doi.org/10.1002/joc.4472
- Malmgren, B. A., Winter, A., & Chen, D. (1998). El Niño-southern Oscillation and North Atlantic Oscillation control of climate in Puerto Rico. Journal of Climate, 11(10), 2713–2717. https://doi.org/10.1175/1520-0442(1998)011<2713:ENOSOA>2.0.CO;2
- Mildner, T. C., Eden, C., & Czeschel, L. (2013). Revisiting the relationship between Loop Current rings and Florida Current transport variability. Journal of Geophysical Research: Oceans, 118(12), 6648–6657. https://doi.org/10.1002/2013JC009109
- Montoya-Sánchez, R. A., Devis-Morales, A., Bernal, G., & Poveda, G. (2018). Seasonal and intraseasonal variability of active and quiescent upwelling events in the Guajira system, southern Caribbean Sea. Continental Shelf Research, 171, 97–112. https://doi.org/10.1016/j.csr.2018.10.006
- Muller-Karger, F. E., Astor, Y. M., Benitez-Nelson, C. R., Buck, K. N., Fanning, K. A., Lorenzoni, L., et al. (2019). The scientific legacy of the CARI-ACO ocean time-series program. *Annual Review of Marine Science*, 11(1), 413–437. https://doi.org/10.1146/annurev-marine-010318-095150
- Müller-Karger, F. E., McClain, C. R., Fisher, T. R., Esaias, W. E., & Varela, R. (1989). Pigment distribution in the Caribbean Sea: Observations from space. *Progress in Oceanography*, 23(1), 23–64. https://doi.org/10.1016/0079-6611(89)90024-4
- Murphy, S. J., Hurlburt, H. E., & O'Brien, J. J. (1999). The connectivity of eddy variability in the Caribbean Sea, the Gulf of Mexico, and the Atlantic ocean. *Journal of Geophysical Research*, 104(C1), 1431–1453. https://doi.org/10.1029/1998JC900010
- Ntaganou, N., Kourafalou, V., Beron-Vera, F. J., Olascoaga, M. J., Le Hénaff, M., & Androulidakis, Y. (2023). Influence of Caribbean eddies on the Loop current system evolution. Frontiers in Marine Science, 10, 961058. https://doi.org/10.3389/fmars.2023.961058
- Oey, L.-Y. (2004). Vorticity flux through the Yucatan Channel and Loop current variability in the Gulf of Mexico. *Journal of Geophysical Research*, 109(C10), C10004. https://doi.org/10.1029/2004JC002400
- Palanisamy, H., Becker, M., Meyssignac, B., Henry, O., & Cazenave, A. (2012). Regional sea level change and variability in the Caribbean sea since 1950. *Journal of Geodetic Science*, 2(2), 125–133. https://doi.org/10.2478/v10156-011-0029-4
- Pedlosky, J. (1987). Geophysical fluid dynamics (2nd ed., p. 710). Springer-Verlag.
- Pratt, R. W., & Maul, G. A. (2000). Sea surface height variability of the intra-Americas Sea from TOPEX/Poseidon satellite altimetry: 1992–1995. Bulletin of Marine Science, 67(2).
- Pujol, M.-I., Faugère, Y., Taburet, G., Dupuy, S., Pelloquin, C., Ablain, M., & Picot, N. (2016). DUACS DT2014: The new multi-mission altimeter data set reprocessed over 20years. Ocean Science, 12(5), 1067–1090. https://doi.org/10.5194/os-12-1067-2016
- Richardson, P. L. (2005). Caribbean Current and eddies as observed by surface drifters. Deep Sea Research Part II: Topical Studies in Oceanography, 52(3–4), 429–463. https://doi.org/10.1016/j.dsr2.2004.11.001
- Sayol, J., Vásquez, L. M., Valencia, J. L., Linero-Cueto, J. R., García-García, D., Vigo, I., & Orfila, A. (2022). Extension and application of an observation-based local climate index aimed to anticipate the impact of El Niño-Southern Oscillation events on Colombia. *International Journal of Climatology*, 42(11), 5403–5429. https://doi.org/10.1002/joc.7540
- Taylor, G. T., Muller-Karger, F. E., Thunell, R. C., Scranton, M. I., Astor, Y., Varela, R., et al. (2012). Ecosystem responses in the southern Caribbean Sea to global climate change. *Proceedings of the National Academy of Sciences*, 109(47), 19315–19320. https://doi.org/10.1073/ pnas.1207514109
- van der Boog, C. G., Jong, M. F., Scheidat, M., Leopold, M. F., Geelhoed, S. C. V., Schulz, K., et al. (2019a). Hydrographic and biological survey of a surface-intensified anticyclonic eddy in the Caribbean Sea. *Journal of Geophysical Research: Oceans*, 124(8), 6235–6251. https://doi.org/10.1029/2018JC014877
- van der Boog, C. G., Pietrzak, J. D., Dijkstra, H. A., Brüggemann, N., van Westen, R. M., James, R. K., et al. (2019b). The impact of upwelling on the intensification of anticyclonic ocean eddies in the Caribbean Sea. *Ocean Science*, 15(6), 1419–1437. https://doi.org/10.5194/
- Wang, C. (2007). Variability of the Caribbean low-level jet and its relations to climate. Climate Dynamics, 29(4), 411–422. https://doi.org/10.1007/s00382-007-0243-z
- Yang, Y., Weisberg, R. H., Liu, Y., & San Liang, X. (2020). Instabilities and multiscale interactions underlying the Loop current eddy shedding in the Gulf of Mexico. *Journal of Physical Oceanography*, 50(5), 1289–1317. https://doi.org/10.1175/JPO-D-19-0202.1
- Yeh, S.-W., Cai, W., Min, S.-K., McPhaden, M. J., Dommenget, D., Dewitte, B., et al. (2018). ENSO atmospheric teleconnections and their response to greenhouse gas forcing. Reviews of Geophysics, 56(1), 185–206. https://doi.org/10.1002/2017RG000568

References From the Supporting Information

- Lellouche, J.-M., Le Galloudec, O., Drévillon, M., Régnier, C., Greiner, E., Garric, G., et al. (2013). Evaluation of global monitoring and fore-casting systems at Mercator Océan. *Ocean Science*, 9(1), 57–81. https://doi.org/10.5194/os-9-57-2013
- Metzger, E. J., Smedstad, O. M., Thoppil, P., Hurlburt, H., Cummings, J., Walcraft, A., et al. (2014). US navy operational global ocean and Arctic ice prediction systems. *Oceanography*, 27, 32–43. https://doi.org/10.5670/oceanog.2014.66

HUANG ET AL. 10 of 10